molecular pharmaceutics

ARTICLE

pubs.acs.org/molecularpharmaceutics

Development of Polymeric Microbubbles Targeted to Prostate-Specific Membrane Antigen as Prototype of Novel Ultrasound Contrast Agents

Vanna Sanna,[*,†] Gianfranco Pintus,[*,‡] Pasquale Bandiera,[‡] Roberto Anedda,[†] Stefania Punzoni,[‡] Bastiano Sanna,[‡] Vincenzo Migaleddu,[§] Sergio Uzzau,[†,‡] and Mario Sechi[*,∥]

[†]Porto Conte Ricerche, Località Tramariglio, 07041, Alghero, Sassari, Italy

[‡]Department of Biomedical Sciences, Centre of Excellence for Biotechnology Development and Biodiversity Research, University of Sassari, 07100 Sassari, Italy

[§]Sardinian Mediterranean Imaging Research Group—no profit foundation, 07100, Sassari, Italy

[∥]Dipartimento di Scienze del Farmaco, University of Sassari, 07100 Sassari, Italy

Supporting Information

ABSTRACT: Ultrasound-targeted microbubbles (MBs) offer new opportunities to enhance the capabilities of diagnostic ultrasound (US) imaging to specific pathological tissue. Herein, we report on the design and development of a novel prototype of US contrast agent based on polymeric MBs targeted to prostate-specific membrane antigen (PSMA) for use in the diagnosis of prostate cancer (PCa). First, a set of air-filled MBs by a variety of biocompatible polymers were prepared and characterized in terms of morphology and echogenic properties after exposure to US. MBs derived from poly(D,L-lactic-*co*-glycolic acid) (PLGA)-poly(ethylene glycol) (PEG) copolymer resulted as the most effective in terms of reflectivity. Such polymer was therefore preconjugated with a urea-based PSMA inhibitor molecular probe (DCL), and the obtained MBs were investigated *in vitro* for their targeting efficacy toward PSMA positive PCa (LNCaP) cells. Fluorescence microscopy proved a specific and efficient adhesion of targeted MBs to LNCaP cells. To our knowledge, this work reports the first model of polymeric MBs appropriately engineered to target PSMA, which might be further optimized and used for PCa diagnosis and potential carriers for selective drug delivery.

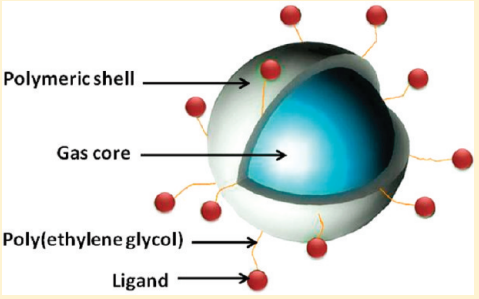

KEYWORDS: targeted microbubbles, biodegradable polymers, ultrasound, contrast agents, prostate cancer, prostate-specific membrane antigen (PSMA)

INTRODUCTION

Ultrasonography is a widely used noninvasive diagnostic medical imaging technique, which is cost-effective and easy to use and provides real-time imaging avoiding the use of hazardous ionizing radiation.[1,2] Ultrasound (US) contrast agents, such as microbubbles (MBs), are providing new opportunities to enhance the diagnostic capabilities of US imaging, because specialized contrast-specific US techniques are able to reveal their nonlinear responses while the linear static ultrasound signals coming from tissues are suppressed. This allows clinicians to obtain information regarding the perfusion behavior of the organs and their diffuse or focal diseases.[3,4]

MBs consist of a specific gas surrounded by a stabilizing shell, with a typical diameter of 1−8 μm, which, intravenously injected in the bloodstream, have the capability to function as blood pool-enhancing agents and to assess tissue blood flow at a microvascular level.[5] With the gas content, shell composition is a key determinant for MBs' physical properties as well as for their acoustic behavior and imaging time.[6] Proposed shell materials, used to prevent gas escaping from the core and to avoid the microbubbles' coalescence,[7] include proteins,[8] lipids,[9] biocompatible polymers[10] and surfactants.[11] The generation of targeted MBs to a specific pathological tissue (for example, neoangiogenesis or tumor antigens) constitutes an emerging field of US contrast agents, as it allows increase of their overall diagnostic potential and, if MBs are loaded with a drug, delivery locally.[12,13] Active targeting usually requires a proper modification of the MB shell to enable selective binding to cellular epitopes or receptors of interest. Ligands belong to various classes of molecules including monoclonal antibodies, polysaccharides and specific peptide sequences that recognize disease antigens.[14−16]

Targeting ligands can be either coincorporated in the shell during MB preparation (i.e., albumin),[15] or attached to the surface of preformulated MBs by covalent or noncovalent methods.[17] In the covalent coupling, the ligand is attached to

Received: October 21, 2010
Accepted: May 5, 2011
Revised: April 11, 2011
Published: May 05, 2011

the headgroup of the material (for example phospholipids) composing the MB shell either directly or *via* a molecular spacer.[18] For noncovalent conjugation, avidin−biotin bridging is a commonly used technique, due to the wide array of available biotinylated ligands and excellent affinity of avidin for biotin.[19,20] By using site labeling to target MBs to specific biomarkers, it has recently been shown that contrast material enhanced US allows detection of specific intravascular molecular markers of tumor angiogenesis,[21,22] thrombosis,[23] inflammation,[24] and breast cancer.[25,26]

In this scenario, we chose prostate cancer (PCa), the second most common cancer in men in the Western countries,[27] as a model disease. Since metastatic PCa is difficult to treat, prevention and/or early detection of premalignant lesions constitute the most effective strategies for minimizing disease related morbidity and mortality. In particular, early diagnosis of PCa is most commonly achieved by digital rectal exam, blood test for prostate specific antigen (PSA), or a prostate biopsy.[28] Despite the successful adoption of these diagnostic modalities for detecting PCa, these are still limited, leaving most early malignancies undiagnosed and sites of metastasis in advanced disease undetected, for which complementary or alternative diagnostic options are needed.

Prostate-specific membrane antigen (PSMA) is a type-II integral membrane protein, predominantly localized in the epithelial cells of the prostate gland and endowed with folate-hydrolase and carboxypeptidase activity.[29] Its low expression in normal prostate epithelial cells increases several fold in high-grade prostate cancers, in metastatic and in androgen-insensitive prostate carcinoma. PSMA is also expressed in the neovasculature of most other solid tumors but not in the vasculature of healthy tissues.[30,31] These features have made it emerge as one of the most attractive biomarkers in the diagnosis, detection, and treatment of PCa.[32,33] The first clinical agent targeting PSMA in PCa was the radionuclide ProstaScint (capromab pendetide, EUSA Pharma),[34] which consists of an intact murine monoclonal antibody, mAb 7E11, labeled with ^{111}In via a linker chelator.[35] The antibody recognizes and binds a cytoplasmatic PSMA epitope, thus only cells with damaged cell membranes can bind mAb 7E11, and this greatly limits the sensitivity of this agent.[36] The most recently developed anti-PSMA mAbs bind to the extracellular domain of PSMA and can be internalized by PSMA-expressing cells.[37,38] However, these radiolabeled monoclonal antibodies tend to produce images that are not easy to interpret. A variety of efforts have been made to develop PSMA-targeted ligands for use in the diagnosis and monitoring of PCa.[39] Above all, a new series of low-molecular-weight, urea-based inhibitors with high affinity and specificity to PSMA, analogous to antibodies and aptamers, have been developed.[40−42]

In this study, we report on the design and development of a novel prototype US contrast agent based on polymeric MBs targeted to PSMA for the use in the diagnosis and, possibly, in the therapy of PCa. In particular, we preliminarily wanted to test whether this specific targeting approach can be successfully applied to MBs, evaluating their interaction in *in vitro* cell assays. This experimental plan can be then used (a) on developing novel prototype with minimal (i.e., optimal) size, in order to cross the vascular compartment and to reach the target tissue, (b) to investigate ultrasonic sonoporation properties of title MBs, and (c) to explore their potential use in enhancing high-intensity focused ultrasound treatment for PCa. Thus, a variety of air-filled biocompatible polymeric MBs, using poly lactic acid (PLA), poly(lactic-*co*-glycolic acid) (PLGA), and PLGA conjugated with poly(ethylene glycol) (PLGA−PEG) were prepared by a double emulsion-solvent evaporation process. Morphology of MBs was studied by scanning electron microscopy (SEM), and the effect of polymers on the reflectivity properties of MBs after exposure to US was explored. With respect to echogenic characteristics, the most responsive MB formulation was then selected as a suitable platform to develop molecularly targeted MBs. The urea-based PSMA inhibitor 2-{[(5-amino-1-carboxypentyl)-carbamoyl]amino}pentanedioic acid,[40,42] hereafter named DCL, was used as a molecular probe, and conjugated with PLGA−PEG polymer before MB preparation. Therefore, using this copolymer (PLGA−PEG−DCL) as starting material,[43] the designed targeted MBs were obtained and characterized (Figure 1). Finally, the adhesion of MBs ligand-functionalized to PSMA positive PCa (LNCaP) cells, as well as a quantitative confirmation of their selective binding, was evaluated *in vitro* by means of fluorescence microscopy and fluorimetric analysis.

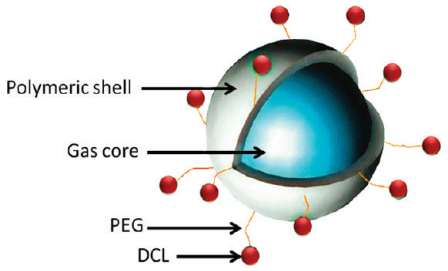

Figure 1. Schematic representation of the designed targeted MBs. The prototype consists of a gas core (air) encapsulated by a shell of PLGA−PEG polymer conjugated to the anti-PSMA ligand DCL.

MATERIALS AND METHODS

Chemicals and Reagents. For the preparation of MBs, poly(D,L-lactide-*co*-glycolide) (PLGA) (lactide:glycolide ratio 50:50, inherent viscosity 0.55−0.75 dL/g in hexafluoroisopropanol) and PLGA (lactide:glycolide ratio 50:50, inherent viscosity 0.20 dL/g in hexafluoroisopropanol) with acid end groups were purchased from Lactel Absorbable Polymers (Pelham, AL, USA). Poly(D,L-lactide) (PLA) (average MW 75,000−120,000; inherent viscosity 0.55−0.75 dL/g in hexafluoroisopropanol), poly(vinyl alcohol) (PVA), 98% hydrolyzed (MW 13000−23000), and fluorescein-5-isothiocyanate (FITC) were obtained from Sigma-Aldrich (Steinheim,Germany). The heterofunctional PEG polymer with a terminal amine and carboxylic acid functional group, NH_2-PEG-COOH (MW 3400), was purchased from JenKem Technology USA. All solvents and other chemicals were obtained from Sigma-Aldrich, Carlo Erba or ORPEGEN Peptide Chemicals GmbH. All reagents of commercial quality were used without further purification.

Instruments. Nuclear magnetic resonance (^{1}H NMR, ^{13}C NMR, HMBC, HSQC, and TOCSY) spectra were determined in $CDCl_3$, DMSO-d_6 or $CDCl_3$/DMSO-d_6 (in 3/1 ratio) and were recorded at 200 MHz, 500 MHz and 600 MHz on a Varian XL-200, a Bruker Avance 500, and a Bruker AMX-600, respectively. Chemical shifts are reported in parts per million (ppm) downfield from tetramethylsilane (TMS), used as an internal standard. Splitting patterns are designated as follows: s, singlet; d, doublet; t, triplet; q, quadruplet; m, multiplet; brs, broad singlet; dd, double doublet. The assignment of exchangeable protons (O*H*

and N*H*) was confirmed by the addition of D_2O. Electron ionization and MALDI TOF mass spectra (70 eV) were recorded on a Hewlett-Packard 5989 mass engine spectrometer and by a MALDI micro MX (Waters, micromass) equipped with a reflectron analyzer. For MALDI TOF mass spectrometry (MS) analysis, the sample was mixed with an equal volume of matrix 2,5-dihydroxybenzoic acid (20 mg/mL in EtOH/H_2O (90:10, v/v), applied to the metallic sample plate and air-dried. Mass calibration was done using as standard the antocyan mixture provided by the manufacturer. Analytical thin-layer chromatography (TLC) was carried out on Merck silica gel F-254 plates. Flash chromatography purifications were performed on Merck Silica gel 60 (230−400 mesh ASTM) as the stationary phase. The purity of copolymers was determined by high performance liquid chromatography (HPLC) using an HP 1200 (Agilent Technologies, USA) system, equipped with a Hypersil BDS C18 column (Alltech Italy, 250 × 4.6 mm i.d., 5 μm particle size); these materials were found to be >95% pure. Elemental analyses for DCL were performed on a Perkin-Elmer 2400 spectrometer at Laboratorio di Microanalisi, Dipartimento di Chimica, Università di Sassari (Italy), and were within ±0.4% of the theoretical values.

Synthesis of PLGA−PEG-COOH. PLGA-COOH (1.5 g, 0.083 mmol) in anhydrous methylene chloride (6 mL) was converted to PLGA−NHS with excess *N*-hydroxysuccinimide (NHS, 38 mg, 0.33 mmol, 4 equiv) in the presence of 1-ethyl-3-(3-dimethylaminopropyl)-carbodiimide (EDC, 70 mg, 0.36 mmol, 4.3 equiv) by magneting stirring at room temperature for 12 h under nitrogen atmosphere. PLGA−NHS was precipitated with cold diethyl ether (5 mL), filtered, repeatedly washed in a cold mixture of diethyl ether and methanol (few drops), and dried with nitrogen and under vacuum to remove solvent (yield: 97%). PLGA−NHS (1.5 g, 0.085 mmol) was dissolved in anhydrous chloroform (5 mL) followed by addition of NH_2-PEG-COOH (0.375 g, 0.11 mmol, 1.3 equiv) and *N*,*N*-diisopropylethylamine (DIPEA) (42 mg, 0.325 mmol, 3.8 equiv), and the reaction mixture was magnetically stirred at room temperature for 24 h. The copolymer was precipitated with cold diethyl ether, and treated with the same solvents to remove unreacted PEG as described above (yield: 88%). The resulting PLGA−PEG block copolymer was dried under vacuum, characterized by ^{1}H NMR (200 and 600 MHz), and used for MB preparation without further treatment. ^{1}H NMR (500 MHz, $CDCl_3$): δ 5.23 (m, −OC−C*H*(CH_3)O−, PLGA), 4.78 (m, −OC−CH_2O-, PLGA), 3.65 (s, −CH_2CH_2O−, PEG), 1.56 (brs, −OC−CHCH_3O−, PLGA).[43]

Preparation of MBs. Polymer coated MBs were fabricated by a modified double water/oil/water (W/O/W) emulsion-solvent evaporation procedure.[44] To generate the first W/O emulsion, 0.2 mL of 1% (w/v) PVA aqueous solution were dispersed in a methylene chloride solution (15 mL) containing 50 mg of polymer (PLA/PLGA/PLGA−PEG) and emulsified (Ultra-Turrax T-25) at 24000 rpm for 5 min. The primary emulsion was then poured into an aqueous 1% (w/v) PVA solution (15.0 mL) and homogenized at 14000 rpm for 5 min in an ice bath, to form the final W/O/W emulsion. The mixture was magnetically stirred in order to evaporate the residual methylene chloride from the generated MBs, and to harden the polymeric shell. The obtained milk-white MB suspension was centrifuged at 1500 rpm for 5 min, washed three times with water, concentrated and stored in glass vials at 4 °C until needed.

Scanning Electron Microscopy. The morphology (shape and surface characteristics) of MBs was investigated using a scanning electron microscopy (SEM, model ESEM-FEI Quanta 200, FEI Company, Hillsboro, OR, USA). Samples were sputter-coated with gold using a vacuum evaporator (Edwards, Milano, Italy) and examined at 25 kV accelerating voltage.

***In Vitro* US Imaging.** To evaluate the inherent echogenicity of different polymeric MBs, *in vitro* preliminary US imaging experiments were performed, similarly to the model reported by Yang et al.[45] Acoustic analysis was carried out by exposing the samples by a self-made acoustic setup. A latex balloon (10 cm diameter) filled with deionized and degassed water was fixed on an anechoic water tank (20 cm long, 15 cm wide, 20 cm deep). Each MB sample, reconstituted in 2.5 mL of saline solution (containing approximately 2.5 × 10^8 bubbles/mL), was then injected with a syringe into the system and insonated using a 512 Sequoia US equipment (Siemens-Acuson, Mountainview, CA, USA) with Cadence contrast pulse sequencing (CPS) software. Technical scanning parameters were as follows: frequency 1.5 MHz, dynamic range 80 dB, temporal resolution between frames 75 and 100 ms (10−13 frames for second), echo-signal gain below noise visibility, signal persistence turned off, and focuses at the level of the middle of self-made acoustic setup. Quantitative analysis of echo-signal intensity was performed on a manually selected region of interest (ROI) by a proprietary software package (Qontrast; e-AMID-Advanced Medical Imaging Development, distributed from Bracco, Milan, Italy).

Synthesis of 2-{[(5-Amino-1-carboxypentyl)carbamoyl]-amino}pentanedioic Acid (DCL). The intermediate (*S*)-2-[3-(5-amino-1-*tert*-butoxycarbonylpentyl)ureido]pentanedioic acid di-*tert*-butyl ester **3** (130 mg, 0.17 mmol, see Supporting Information for ^{1}H-1D NMR, ^{1}H−^{1}H COSY, ^{1}H−^{13}C HMBC, ^{1}H−^{13}C HSQC, and ^{1}H−^{1}H TOCSY spectra, Figures S1−S5 in the Supporting Information) was dissolved in 5 mL of 1:1 (v/v) trifluoroacetic acid (TFA):methylene chloride solution and stirred at room temperature for 3 h. Then, the resulting solution was evaporated under reduced pressure. The colorless solid residue was triturated with dry diethyl ether, filtered, and washed with dry diethyl ether to yield the desired product (yield: 70%) as an off beige solid. The ^{1}H NMR spectra was in accordance with that reported in literature.[43] MS (MALDI-TOF): [M^+ 319]; [M^+ 319 + Na, 342]. EI: [M^+ 319]. Anal. ($C_{12}H_{21}N_3O_7$·1.15CF_3COOH) C, H, N.

Preparation of DCL-Conjugate Copolymer (PLGA−PEG−DCL). To PLGA−PEG-COOH diblock copolymer (1.4 g, 0.065 mmol) in anhydrous methylene chloride under nitrogen (5 mL), NHS (30 mg, 0.26 mmol, 4 equiv) and EDC (53 mg, 0.26 mmol, 4.3 equiv) were added, and the solution was stirred at room temperature for 12 h. The activated PLGA−PEG-NHS copolymer was recovered by precipitation in ice-cold diethyl ether, and methanol (few drops), filtered and dried with nitrogen and then under vacuum to remove residual solvents (yield: 92%). The PLGA−PEG-NHS (0.45 g, 0.022 mmol) in dimethylformamide (DMF, 2.5 mL) was reacted with a solution of DCL salt (38 mg, 0.088 mmol, 4 equiv) in DMF (1 mL) in the presence of DIPEA (0.72 mL, 0.0041 mol) for 24 h at room temperature under nitrogen. The obtained PLGA−PEG−DCL was analyzed by high performance liquid chromatography (HPLC) on a Hypersil BDS C18 column (Alltech Italy), (250 × 4.6 mm i.d., 5 μm particle size), using as eluent a linear gradient of eluent B (95% MeCN, 0.07% TFA) in A (0.1% TFA) from 15 to 100% for 30 min (flow rate 1 mL/min, temperature at

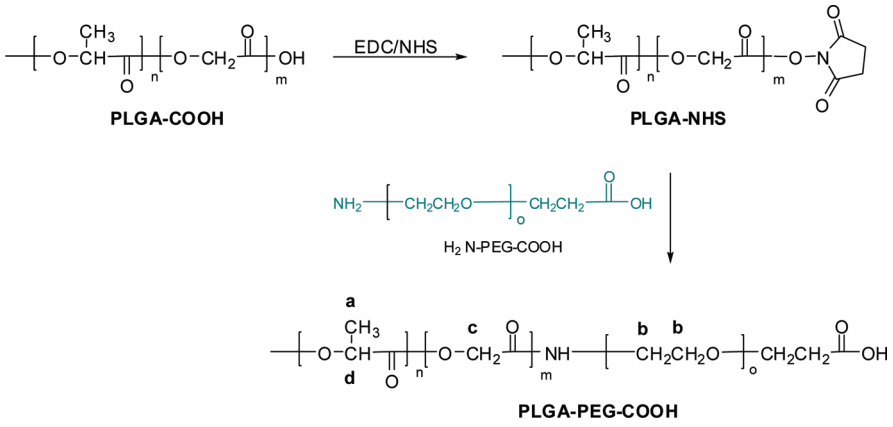

Figure 2. Synthesis of PLGA−PEG-COOH.

25 °C and a detector wavelength of 280 nm). The equipment consisted of an HP 1200 (Agilent Technologies, USA) system, controlled by the HP ChemStation software, including an autosampler and a diode array detector. After purification, characterization of the obtained white solid (yield: 65%) was assessed by ^{1}H NMR, and the spectrum was in accordance with that reported in the literature.[43] The polymer was then freeze-dried and stored at −20 °C.

Preparation and Characterization of Nontargeted and Targeted FITC-Loaded MBs. Dye-encapsulated MBs containing fluorescein-5-isothiocyanate (FITC) were prepared using the PLGA−PEG and PLGA−PEG−DCL conjugated polymers. Nontargeted and targeted FITC-loaded MBs were obtained using the W/O/W method as described above, by addition of a 1% (w/v) PVA solution (0.2 mL) containing FITC (7.5 mg/mL) to the organic polymer solution. Before use, the MBs were characterized by SEM analysis.

Cell Culture and *in Vitro* Adhesion of MBs. The prostate LNCaP cell lines (ECACC, Salisbury, U.K.) were grown in glass chamber slides (Nunc, Rochester, NY) with RPMI 1640 medium, containing 100 units/mL penicillin G, 100 μg/mL streptomycin and 10% FBS (Invitrogen, Carlsbad, CA), at concentrations allowing 70% confluence in 24 h. On the day of experiments, cells were washed with PBS and then exposed for 30 min to both targeted and nontargeted FITC-loaded MBs (1.5 mg/mL) in 1 mL of serum-free culture medium. After MB incubation, cells were washed three times with PBS, fixed with 4% paraformaldehyde, counterstained with Hoechst (10 μg/mL) (Invitrogen, Carlsbad, CA), mounted and visualized by fluorescence microscopy (Olympus IX70) in order to evaluate the interaction of MBs with LNCaP cells. For each sample, the FITC positive population was assessed by enumeration of green labeled cells in each sample for a minimum of six random fields per sample viewed at 100× magnification. Results were expressed as number of cells per field (mean ± SD) in groups.

Fluorimetric Quantitative Analysis of FITC-Positive Cells. Quantitative analysis of green-positive cells exposed to both targeted and nontargetd FITC-loaded MBs was assessed as previously described[46] with minor modification by using FITC/Hoechst double fluorescent staining. Hoechst is a dye that is able to stain the nuclei of all cells, whether they have or have not interacted with the employed MBs. Thus all nuclei could be recognized by the blue fluorescence of Hoechst, while only cells that have interacted with FITC-loaded MBs fluoresced green due to the cell-associated FITC. LNCaP cells were grown in 24-well plates (BD Falcon, Franklin Lakes, NJ), at concentrations allowing 70% confluence in 24 h. On the day of experiments, cells were washed with PBS and then exposed for 30 min to both targeted and nontargeted FITC-loaded MBs (1.5 mg/mL) in 1 mL of serum-free culture medium. After MB incubation, cells were washed three times with PBS, and then stained with Hoechst (10 μg/mL) (Invitrogen), washed with PBS again and fluorescence measured by using a GENios plus microplate reader (Tecan). Excitation and emission wavelengths used for fluorescence quantification were, respectively, 340 and 485 nm for Hoechst and 485 and 535 nm for FITC. Results were expressed as percent of the ratio (FITC/Hoechst) concerning the relative fluorescence units (RFU) of two dyes reads.

Statistical Analysis. The data were processed and analyzed by Origin software (version 7.0 SR0, OriginLab Corporation, USA). The statistical analysis was evaluated by a Student's *t*-test, and *p*-values <0.05 were considered statistically significant. All data reported are means ± standard deviation (SD), unless otherwise specified.

RESULTS AND DISCUSSION

Preparation of PLGA−PEG-COOH Copolymer. In addition to the other materials (PLA and PLGA), we chose PLGA−PEG-COOH as a polymer system because of its well-established safety in clinical use, and by considering its already discussed biocompatible properties.[47] In our case, pegylation served not only to preserve the antibiofouling properties[48] of MB construct but also as a spacer in order to maintain sufficient distance between the PSMA inhibitor and the MB surface. In fact, according to the solved 3.5 Å crystal structure of the PSMA ectodomain,[49,50] the active site, which contains a binuclear zinc site and the catalytic residues, was located by a funnel-shaped tunnel with a depth of approximately 20 Å and a width of 8−9 Å. To enable high-affinity binding of our prototypes to PSMA, we planned to attach a functionalized >20 Å polymethylene linker (PEG) to the amino functionality of the lysine moiety of the DLC. Therefore, part of the linker portion of the polymeric fragment should remain outside of the 20 Å tunnel as long as the glutamate moiety is maintained within the binding pocket, thus permitting a putative strong interaction between the inhibitor and PSMA. The starting carboxylate-functionalized diblock copolymer PLGA−PEG-COOH (Figure 2) was synthesized

dx.doi.org/10.1021/mp100360g |*Mol. Pharmaceutics* 2011, 8, 748–757

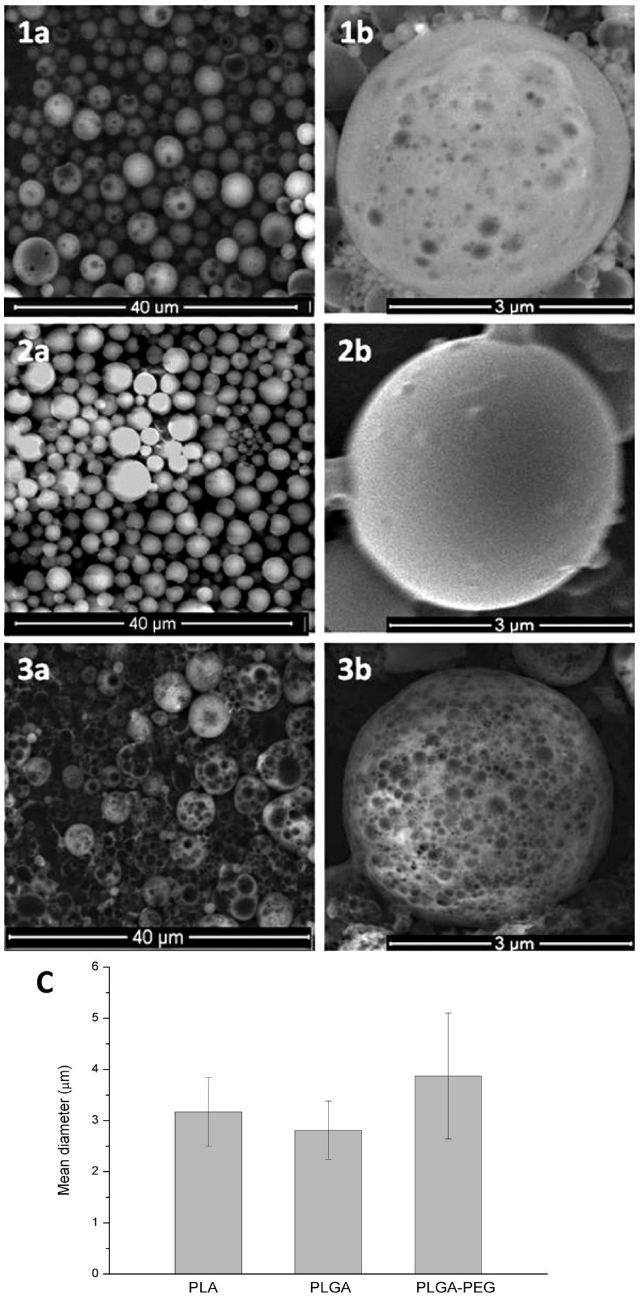

Figure 3. Scanning electron microscopy images of PLA- (1), PLGA- (2) and PLGA−PEG- (3) based MBs samples at (a) low and (b) high magnification; (c) mean diameter ± standard deviation (SD) of PLA-, PLGA-, and PLGA−PEG-COOH-based MBs.

by conjugating NH_2-PEG-COOH to PLGA-COOH, following a modified described procedure.[51,52,43] The basic chemical structure of the copolymer was confirmed by ^{1}H NMR spectroscopy. Interestingly, a large peak at 3.65 ppm, corresponding to the PEG methylene protons, was detected. In fact, analysis of proton intensities, used for determination of the composition of the copolymers, revealed an increased efficacy of PEG conjugation to PLGA (PLGA/PEG approximately in 1:1.5 molar ratio), as previously described.[52] We confirmed that the optimal combination of parameters resulted when final coupling reaction was carried out using $CHCl_3$ as a solvent, and stirred for 24 h. As far as the full characterization is concerned, overlapping doublets detected at 1.56 ppm are attributed to the lactide methyl repeat units. The multiplets (quartets) at 5.23 and 4.78 ppm correspond to the lactide methine (CH) and the glycolide protons (CH_2), respectively, with a high complexity of the peaks resulting from different D-lactic, L-lactic, glycolic acid sequences in the polymer backbone.

Characterization of MBs. In this study, air-filled MBs with a polymeric shell (PLA, PLGA and PLGA−PEG) were formulated by W/O/W emulsion-solvent evaporation process. These polymers have been chosen because they offer several advantages, such as high biocompatibility and long circulation time, and enable the formation of a rigid shell that still allows for resonance and harmonic imaging.[10,53] We predicted that the inherent surface properties of the MB shell are strongly related to physicochemical parameters of the polymer used (molecular weight, crystallinity, and the terminal groups), and this can play a fundamental role for the US echo contrast (see below). The morphology and particle size for each batch of MBs were evaluated by SEM analysis. As reported in Figure 3, SEM photomicrographs showed that double emulsion formulation produces constructs with a spherical shape but different morphologies.

In particular, PLA-based MBs were characterized by the presence of some vesicular structures entrapped in the outer polymeric shell. On the other hand, PLGA-based MBs presented a smooth and regular surface. A distinctive closed honeycomb structure was detected for the PLGA−PEG-based construct, which showed an irregular surface. This is probably due to polymer precipitation around the numerous inner emulsion microdroplets, which were present on the entire particle structure. The origin of MBs having different morphology is attributable to the emulsion droplets with different content of inner aqueous phase that, in our case, can be related to the different hydrophilicity of the polymers used. For example, PLA polymer bearing carboxylic acid function terminal groups is more hydrophilic with respect to the PLGA with ester end groups, whereas the addition of poly(ethylene glycol) (PEG) chains markedly improves the hydrophilic properties of the block copolymers. Thus, using hydrophilic polymers, the diameter of the inner microdroplets resulted much smaller than that of the emulsion droplets, and as such the formation of honeycomb structures is favored.[54]

The size of MBs is an important parameter to control, because they should have a diameter ranging from 2 to 8 μm, to be able to transit via normal pulmonary and systemic capillary beds.[17] As reported in Figure 3C, the double emulsion−evaporation preparation method used ensures an appropriate size distribution of MBs, with an average diameter of about 3−4 μm.

***In Vitro* US Imaging of MBs.** A preliminary evaluation of different polymeric MBs as US contrast agents was performed by measuring the enhancement of the US image in terms of reflectivity. The MBs represent strong reflectors of sound and thus generate brightness on the US image.[55] The US imaging of deionized water (used as a control), PLA-, PLGA-, and PLGA−PEG-based MBs is shown in Figure 4. Compared with water (Figure 4A), the brighter area can be distinctly seen in the tested MBs (Figures 4B−D). Each prototype displayed a different brightness depending on the polymeric shell composition.

To determine the change in signal for each MB formulation, US signal intensity was quantified, and the corresponding mean percentage values within the ROIs are shown in Figure 4E. Results confirmed that all polymeric MBs contributed to

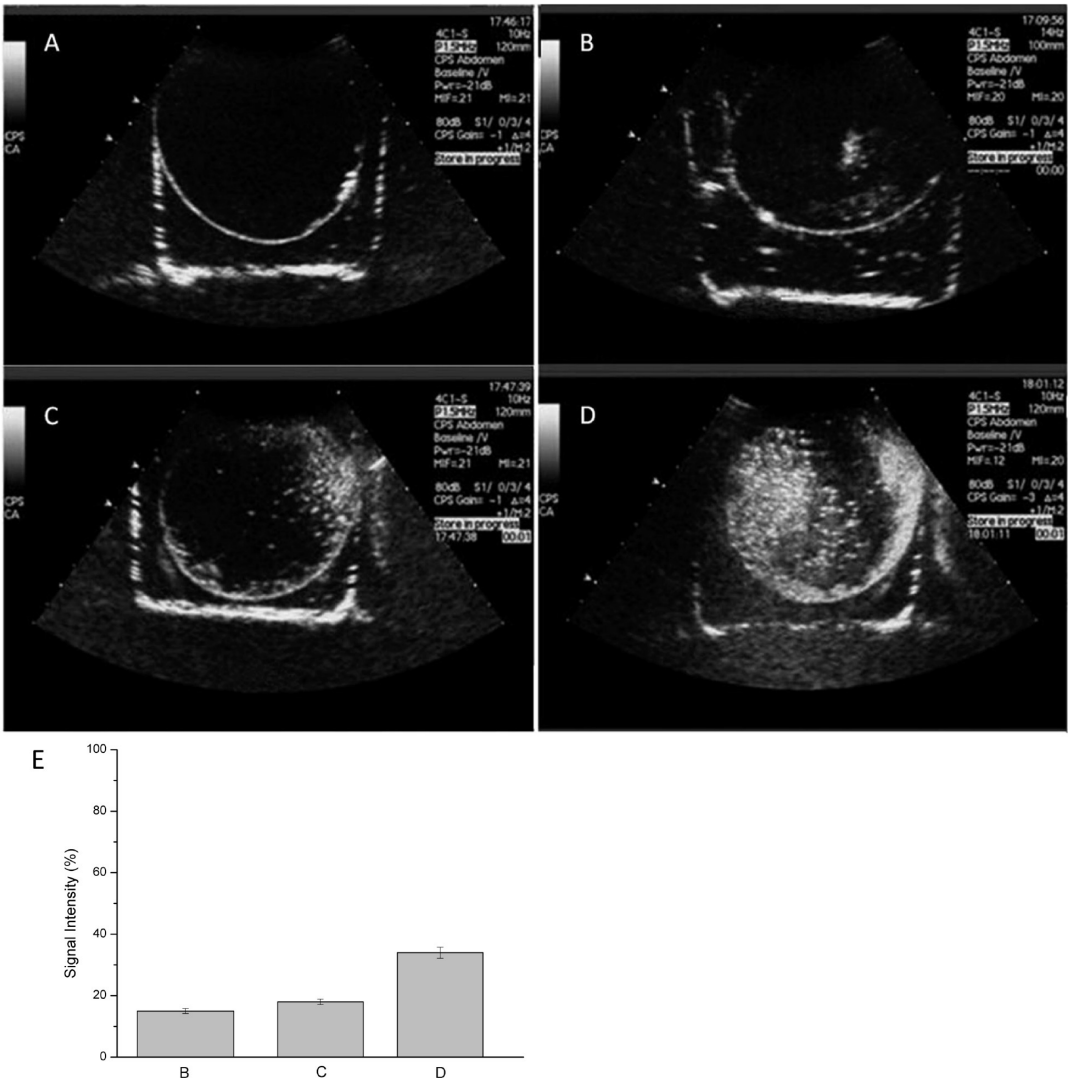

Figure 4. The *in vitro* ultrasound imaging in the different samples: (A) degassed and deionized water, (B) PLA-, (C) PLGA-, and (D) PLGA−PEG-based MBs. (E) Quantitative analysis of echo-signal intensity ± SD within ROI corresponding to US images.

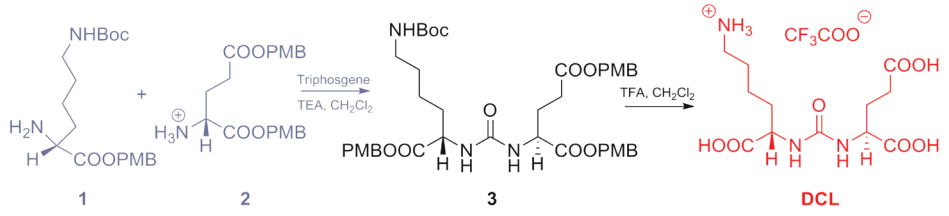

Figure 5. Synthesis of DCL.

ultrasound reflected echo intensity with respect to water. The signal intensity increased significantly ($p < 0.05$) in the order PLA < PLGA < PLGA−PEG and resulted as 15 ± 0.08, 18 ± 0.9 and 34 ± 1.8%, respectively. Furthermore, among the investigated formulations, the PLGA−PEG-based MBs gave better contribution to ultrasound echo effect. Therefore, such prototype was selected for the next step of this work, focused on targeting studies.

Preparation of DCL. We strategically selected an inhibitor containing lysine, DCL (Figure 5), which is ideally suited for this purpose, due to the presence of a primary amine that allows for amide bond formation with carboxyl groups present on PEG monomers. As above-mentioned, this probe derives from a series of PSMA inhibitors, also developed as low-molecular-weight radiopharmaceutical-based imaging agents. We sought to obtain DCL from the urea-based intermediate **3** (Figure 5), previously reported by Pomper's group.[42,56] It is worth nothing that the preparation of this key compound has also been revisited by us, and has been presented elsewhere.[43] Briefly, **3** was synthesized by treating bis-4-methoxybenzyl-L-glutamate·HCl (**2**) with

triphosgene and TEA at 0 °C, followed by addition of 2-amino-6-*tert*-butoxycarbonylamino-hexanoic acid 4-methoxybenzyl ester (**1**). Both synthones **1** and **2** were prepared according to previously described procedures.[56,57] Focusing on the final step reaction, both the *tert*-butyloxycarbonyl (Boc) and the *p*-methoxybenzyl (PMB) groups of **3** were conveniently removed at room temperature by using a TFA/CH_2Cl_2 solution.

Synthesis and Characterization of PLGA−PEG−DCL. To address the device to the targeted organ, a suitable functionalization of the MB polymeric shell should be envisioned. We propose to develop targeted MBs by the self-assembly of an amphiphilic pseudo-triblock copolymer composed of end-to-end linkage of PLGA, PEG and the DCL as targeting moiety, which would bind to the PSMA on the surface of PCa cells. The strategy of block copolymers has been previously proposed for targeted nanoparticle−aptamer bioconjugates for cancer therapy by Farokhzad's group.[51] As above-mentioned, the presence of PEG chains is especially desirable because pegylated polymeric particles have significantly reduced systemic clearance and minimizes the particle uptake by nontargeted cells.[58] Moreover, we chose to develop new prefunctionalized biomaterials that have all of the desired MB components to avoid post-particle modifications. This synthetic approach results in precisely engineered MBs, which can be able to reduce the batch-to-batch variations in their biophysicochemical properties.[51] The PLGA−PEG−DCL copolymer was synthesized by using the already described two-step reaction. The carboxy-terminal PLGA−PEG-COOH was activated with NHS, to form the intermediate PLGA−PEG-NHS, and then conjugated to the amine functional group of the DCL, thus providing PLGA−PEG−DCL as a pseudo-triblock copolymer (Figure 6, stage 1). In addition to the resonance shifts (a−d, Figure S6, Supporting Information) of the PLGA−PEG framework, the corresponding ^{1}H NMR spectra recorded for PLGA−PEG−DCL exhibited a series of partially overlapped multiple peaks, attributable to the pattern signals of DCL.[43] In particular, multiplets in the range of 2.78−2.72 and 2.00−1.85 ppm resonance, characteristic of the aliphatic backbone of DCL, were clearly observed.

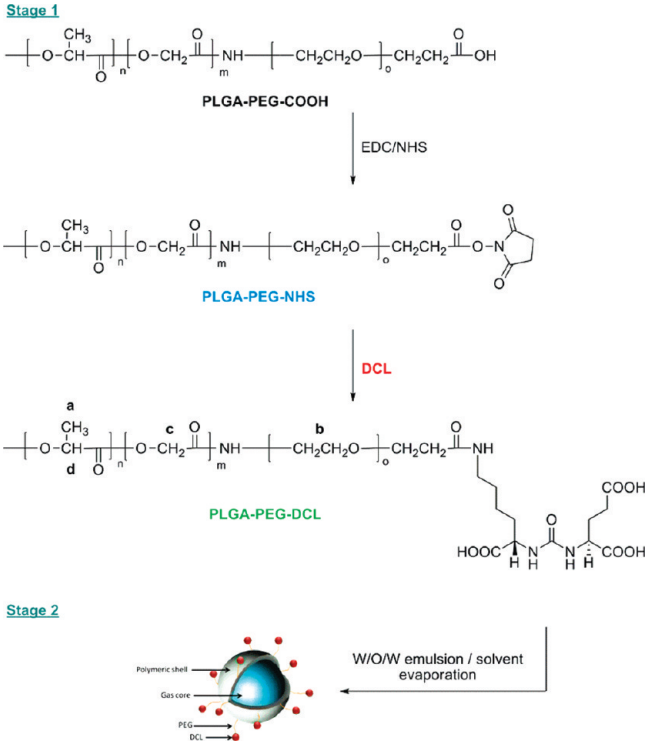

Figure 6. Stage 1: preparation of PLGA−PEG−DCL polymer. Stage 2: preparation of targeted MBs.

Characterization of Nontargeted and Targeted FITC-Loaded MBs. To obtain a set of nontargeted and targeted air-filled FITC-loaded MBs, the W/O/W emulsion-solvent evaporation process was used (Figure 6, stage 2), according with the above-described procedure. The use of PLGA−PEG copolymer conjugated with DCL as well as the loading with FITC into MBs did not determine significant change in the morphology and size (Figure 7), which resulted to be similar to those observed (within a diameter range of 3−4 μm) for PLGA−PEG-based MBs.

***In Vitro* Studies of MBs on Tumor Cells.** The PSMA is highly expressed on virtually all PCa cells and is currently the focus of several diagnostic and therapeutic strategies.[28] LNCaP human prostate epithelial cells express a high level of PSMA protein on their surface and represent a good model for *in vitro* and *in vivo* PCa studies.[59] In this context, the potential selective adhesion of targeted MBs to LNCaP cells was investigated by fluorescence microscopy. Untreated control cell and cells exposed to both targeted and nontargeted FITC-encapsulated MBs were explored as comparison. Fluorescence images taken after 30 min of LNCaP cells exposed to MBs samples are shown in Figure 8.

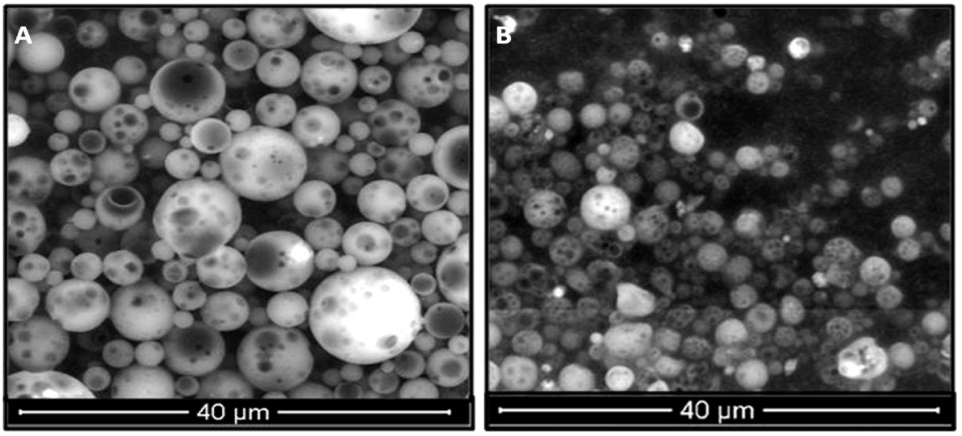

Figure 7. Scanning electron microscopy images of nontargeted (A) and targeted (B) FITC-loaded MBs.

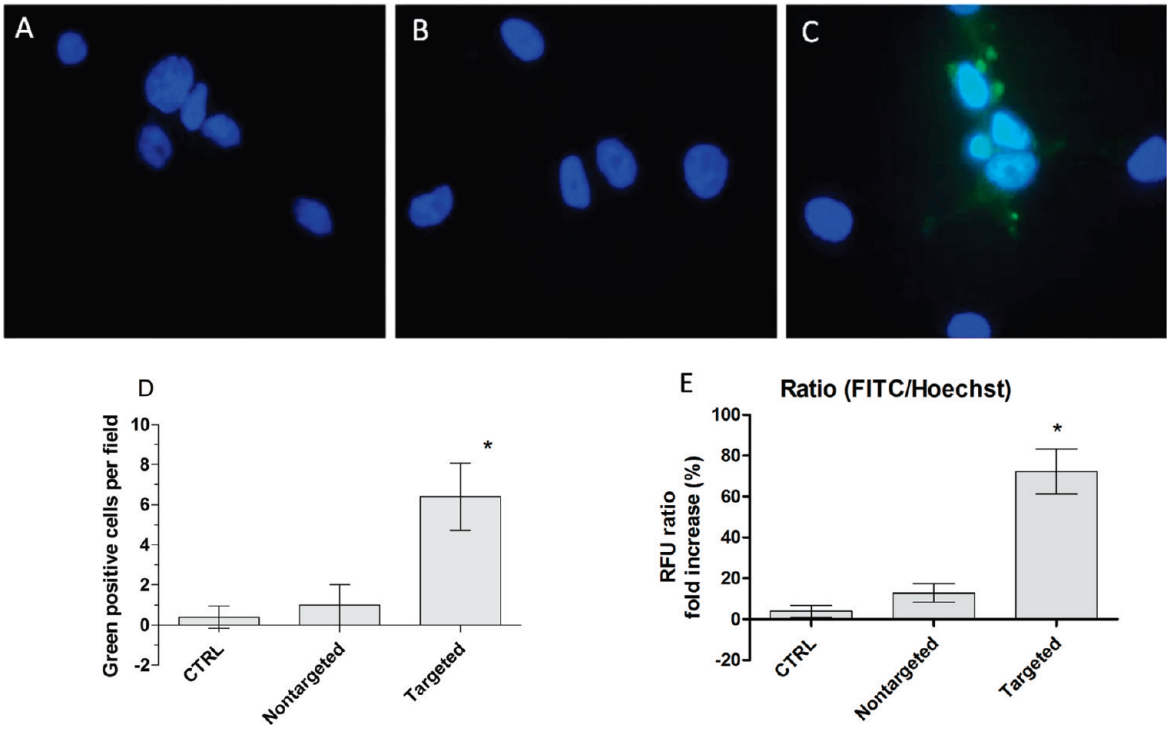

Figure 8. Representative fluorescence images (100× magnification) of LNCaP (PSMA+) PCa cells. Untreated control (A), after 30 min of exposure to nontargeted FITC-loaded (B), and targeted FITC-loaded (C) MBs. The cell nuclei were stained with Hoechst (blue). Number of green-positive cells per field (mean ± SD) in the three different groups (D). *Significantly different from nontargeted MBs. (E) Fluorimetric quantitative analysis of FITC-positive cells. Fluorimetric quantification of green positive cells by FITC−Hoechst double staining. Data are expressed as percent of the ratio (FITC/Hoechst) concerning the relative fluorescence units (RFU) of two dyes reads. *Significantly different from nontargeted MBs ($P < 0.05$, $n = 3$).

No noticeable variation of fluorescence intensity between the control (Figure 8A) and with nontargeted MBs treated cells (Figure 8B) was revealed. Conversely, a large amount of cell-associated green fluorescence was observed after the exposure of LNCaP cells to targeted MBs (Figure 8C), thus indicating their significant cellular adhesion (Figure 8D). Further quantitative confirmation of the selective binding exerted by targeted FITC-encapsulated MBs toward PSMA-positive LNCaP cells is depicted in Figure 8E. These results indicate that functionalization of the MB surface with the selective PSMA ligand DCL efficiently promotes their adhesion with LNCaP cells in comparison to the unfunctionalized ones.

CONCLUSIONS

In this work, we have shown that the W/O/W emulsion technique can be successfully applied for the formulation of air-filled MBs based on different biodegradable polymers as US contrast agents. Such a method resulted to be able to generate particles with a controlled diameter on the desired sub-micrometer range. We also found that polymer composition dramatically influenced the morphological characteristics of MBs as well as their echogenicity during insonation. Moreover, to formulate targeted MBs, a novel approach based on PLGA−PEG preconjugation with an anti-PSMA probe has been well performed. We demonstrated that, with respect to the corresponding nontargeted prototype, the targeted MBs bind specifically and efficiently to PSMA positive PCa (LNCaP) cells, thus offering a potential improvement in terms of selectivity. In summary, this study provides novel insights that might be useful to improve the efficiency of US contrast agents, and to allow simultaneous PCa imaging and targeted drug delivery. We hope these results might constitute a suitable platform for development of powerful diagnostic and therapeutic tools addressed toward several other target diseases.

ASSOCIATED CONTENT

Supporting Information. Figures S1−S6: ^{1}H-1D NMR (S1), ^{1}H−^{1}H COSY (S2), ^{1}H−^{13}C HMBC (S3), ^{1}H−^{13}C HSQC (S4), and ^{1}H−^{1}H TOCSY (S5) spectra of intermediate **3** recorded in $CDCl_3$ at 600 MHz; ^{1}H NMR with pattern signals of PLGA−PEG and of DCL (S6). This material is available free of charge via the Internet at http://pubs.acs.org.

AUTHOR INFORMATION

Corresponding Author

*V.S.: Porto Conte Ricerche, Località Tramariglio, 07041, Alghero, Sassari, Italy; tel, +39 079-998-619; fax, +39 079-228-720; e-mail, sannav@portocontericerche.it. G.P.: Department of Biomedical Sciences, University of Sassari, Centre of Excellence for Biotechnology Development and Biodiversity Research, Viale San Pietro 43/B, 07100 Sassari, Italy; tel, +39 079-228-121; fax, +39 079-228-120; e-mail, gpintus@uniss.it. M.S.: Dipartimento di Scienze del Farmaco, University of Sassari, Via Muroni 23/A, 07100 Sassari, Italy; tel, +39 079-228-753; fax, +39 079-228-720; e-mail: mario.sechi@uniss.it.

■ ACKNOWLEDGMENT

The research activities presented were done within the frame of "Progetto Cluster – Sviluppo ed Utilizzo di Nanodevices", funded by Sardinian Technology Park - Porto Conte Ricerche, Italy. The authors thank Alessandro Arca for the preparation of the polymers and ligand DCL.

■ REFERENCES

(1) Willmann, J. K.; van Bruggen, N.; Dinkelborg, L. M.; Gambhir, S. S. Molecular imaging in drug development. *Nat. Rev. Drug Discovery* **2008**, *7*, 591–607.

(2) Rapoport, N.; Kennedy, A. M.; Shea, J. E.; Scaife, C. L.; Nam, K. H. Ultrasonic nanotherapy of pancreatic cancer: lessons from ultrasound imaging. *Mol. Pharmaceutics* **2010**, *7*, 22–31.

(3) Lindner, J. R. Microbubbles in medical imaging: current applications and future directions. *Nat. Rev. Drug Discovery* **2004**, *3*, 527–532.

(4) Cosgrove, D. Ultrasound contrast agents: an overview. *Eur. J. Radiol.* **2006**, *60*, 324–330.

(5) Hernot, S.; Klibanov, A. L. Microbubbles in ultrasound-triggered drug and gene delivery. *Adv. Drug Delivery Rev.* **2008**, *60*, 1153–1166.

(6) Cavalieri, F.; Ashokkumar, M.; Grieser, F.; Caruso, F. Ultrasonic Synthesis of Stable, Functional Lysozyme Microbubbles. *Langmuir* **2008**, *24*, 10078–10083.

(7) Xing, Z.; Ke, H.; Wang, J.; Zhao, B.; Yue, X.; Dai, Z.; Liu, J. Novel ultrasound contrast agent based on microbubbles generated from surfactant mixtures of Span 60 and polyoxyethylene 40 stearate. *Acta Biomater.* **2010**, *6*, 3542–3549.

(8) Barnhart, J.; Levene, H.; Villapando, E.; Maniquis, J.; Fernandez, J.; Rice, S.; Jablonski, E.; Gjøen, T.; Tolleshaug, H. Characteristics of Albunex: air-filled albumin microspheres for echocardiography contrast enhancement. *Invest. Radiol.* **1990**, *25* (Suppl. 1), S162–164.

(9) Ferrara, K. W.; Borden, M. A.; Zhang, H. Lipid-shelled vehicles: engineering for ultrasound molecular imaging and drug delivery. *Acc. Chem. Res.* **2009**, *42*, 881–892.

(10) El-Sherif, D. M.; Wheatley, M. A. Development of a novel method for synthesis of a polymeric ultrasound contrast agent. *J. Biomed. Mater. Res. A* **2003**, *66*, 347–355.

(11) Krupka, T. M.; Solorio, L.; Wilson, R. E.; Wu, H.; Azar, N.; Exner, A. A. Formulation and Characterization of Echogenic Lipid-Pluronic Nanobubbles. *Mol. Pharmaceutics* **2010**, *7*, 49–59.

(12) Sakamoto, J. H.; Smith, B. R.; Xie, B.; Rokhlin, S. I.; Lee, S. C.; Ferrari, M. The molecular analysis of breast cancer utilizing targeted nanoparticle based ultrasound contrast agents. *Technol. Cancer Res. Treat.* **2005**, *4*, 627–636.

(13) Quaia, E. Microbubble ultrasound contrast agent: an update. *Eur. J. Radiol.* **2007**, *17*, 1995–2008.

(14) Pillai, R.; Marinelli, E. R.; Fan, H.; Nanjappan, P.; Song, B.; von Wronski, M. A.; Cherkaoui, S.; Tardy, I.; Pochon, S.; Schneider, M.; Nunn, A. D.; Swenson, R. E. A Phospholipid-PEG2000 Conjugate of a Vascular Endothelial Growth Factor Receptor 2 (VEGFR2)-Targeting Heterodimer Peptide for Contrast-Enhanced Ultrasound Imaging of Angiogenesis. *Bioconjugate Chem.* **2010**, *21*, 556–562.

(15) Korpanty, G.; Grayburn, P. A.; Shohet, R. V.; Brekken, R. A. Targeting vascular endothelium with avidin microbubbles. *Ultrasound Med. Biol.* **2005**, *31*, 1279–1283.

(16) Weller, G. E.; Wong, M. K.; Modzelewski, R. A.; Lu, E.; Klibanov, A. L.; Wagner, W. R.; Villanueva, F. S. Ultrasonic imaging of tumor angiogenesis using contrast microbubbles targeted via the tumor-binding peptide arginine-argininele ucine. *Cancer Res.* **2005**, *65*, 533–539.

(17) Lindner, J. R. Molecular imaging of cardiovascular disease with contrast-enhanced ultrasonography. *Nat. Rev. Cardiol.* **2009**, *6*, 475–481.

(18) Kim, D. H.; Klibanov, A. L.; Needham, D. The influence of tiered layers of surface-grafted poly(ethylene glycol) on receptor–ligand-mediated adhesion between phospholipid monolayer-stabilized microbubbles and coated glass beads. *Langmuir* **2000**, *16*, 2808–2817.

(19) Mayer, C. R.; Bekeredjian, R. Ultrasonic gene and drug delivery to the cardiovascular system. *Adv. Drug Delivery Rev.* **2008**, *60*, 1177–1192.

(20) Böhmer, M. R.; Klibanov, A. L.; Tiemann, K.; Hall, C. S.; Gruell, H.; Steinbach, O. C. Ultrasound triggered image-guided drug delivery. *Eur. J. Radiol.* **2009**, *70*, 242–253.

(21) Willmann, J. K.; Cheng, Z.; Davis, C.; Lutz, A. M.; Schipper, M. L.; Nielsen, C. H.; Gambhir, S. S. Targeted Microbubbles for Imaging Tumor Angiogenesis: Assessment of Whole-Body Biodistribution with Dynamic Micro-PET in Mice. *Radiology* **2008**, *249*, 212–219.

(22) Reinhardt, M.; Hauff, P.; Linker, R. A.; Briel, A.; Gold, R.; Rieckmann, P.; Becker, G.; Toyka, K. V.; Mäurer, M.; Schirner, M. Ultrasound derived imaging and quantification of cell adhesion molecules in experimental autoimmune encephalomyelitis (EAE) by sensitive particle acoustic quantification (SPAQ). *Neuroimage* **2005**, *27*, 267–278.

(23) Schumann, P. A.; Christiansen, J. P.; Quigley, R. M.; McCreery, T. P.; Sweitzer, R. H.; Unger, E. C.; Lindner, J. R.; Matsunaga, T. O. Targeted-microbubble binding selectively to GPIIb IIIa receptors of platelet thrombi. *Invest. Radiol.* **2002**, *37*, 587–593.

(24) Lindner, J. R.; Dayton, P. A.; Coggins, M. P.; Ley, K.; Song, J.; Ferrara, K.; Kaul, S. Non-invasive assessment of inflammation using ultrasound detection of phagocytosed microbubbles. *Circulation* **2000**, *102*, 531–538.

(25) Chappell, J. C.; Price, R.J. Targeted therapeutic applications of acoustically active microspheres in the microcirculation. *Microcirculation* **2006**, *13*, 57–70.

(26) Bloch, S. H.; Dayton, P.; Ferrara, K. W. Targeted imaging using ultrasound contrast agents. Progess and opportunities for clinical and research applications. *IEEE Eng. Med. Biol. Mag.* **2004**, *23*, 18–29.

(27) Jemal, A.; Siegel, R.; Xu, J.; Ward, E. Cancer statistics 2008. *Ca-Cancer J. Clin.* **2008**, *58*, 71–96.

(28) Kularatne, S. A.; Wang, K.; Santhapuram, H. K. R.; Low, P. S. Prostate-Specific Membrane Antigen Targeted Imaging and Therapy of Prostate Cancer Using a PSMA Inhibitor as a Homing Ligand. *Mol. Pharmaceutics* **2009**, *6*, 780–789.

(29) Rajasekaran, A. K.; Anilkumar, G.; Christiansen, J. J. Is prostate-specific membrane antigen a multifunctional protein?. *Am. J. Physiol.* **2005**, *288*, C975–981.

(30) Ghosh, A.; Heston, W. D. Tumor target prostate specific membrane antigen (PSMA) and its regulation in prostate cancer. *J. Cell. Biochem.* **2004**, *91*, 528–539.

(31) Chang, S. S.; O'Keefe, D. S.; Bacich, D. J.; Reuter, V. E.; Heston, W. D.; Gaudin, P. B. Prostate-specific membrane antigen is produced in tumor-associated neovasculature. *Clin. Cancer Res.* **1999**, *5*, 2674–2681.

(32) Colombatti, M.; Grasso, S.; Porzia, A.; Fracasso, G.; Scupoli, M. T.; Cingarlini, S.; Poffe, O.; Naim, H. Y.; Heine, M.; Tridente, G.; Mainiero, F.; Ramarli, D. The prostate specific membrane antigen regulates the expression of IL-6 and CCL5 in prostate tumour cells by activating the MAPK pathways. *PLoS One* **2009**, *4*, e4608.

(33) Wolf, P.; Freudenberg, N.; Bühler, P.; Alt, K.; Schultze-Seemann, W.; Wetterauer, U.; Elsässer-Beile, U. Three conformational antibodies specific for different PSMA epitopes are promising diagnostic and therapeutic tools for prostate cancer. *Prostate* **2010**, *70*, 562–569.

(34) Elsässer-Beile, U.; Bühler, P.; Wolf, P. Targeted therapies for prostate cancer against the prostate specific membrane antigen. *Curr. Drug Targets* **2009**, *10*, 118–125.

(35) Apolo, A. B.; Pandit-Taskar, N.; Morris, M. J. Novel tracers and their development for the imaging of metastatic prostate cancer. *J. Nucl. Med.* **2008**, *49*, 2031–2041.

(36) Troyer, J. K.; Beckett, M. L.; Wright, G. L., Jr. Detection and characterization of the prostate-specific membrane antigen (PSMA) in tissue extracts and body fluids. *Int. J. Cancer* **1995**, *62*, 552–558.

(37) Nargund, V.; Al Hashmi, D.; Kumar, P.; Gordon, S.; Otitie, U.; Ellison, D.; Carroll, M.; Baithun, S.; Britton, K. E. Imaging with radiolabelled monoclonal antibody (MUJ591) to prostate-specific membrane antigen in staging of clinically localized prostatic carcinoma: comparison with clinical, surgical and histological staging. *BJU Int.* **2005**, *95*, 1232–1236.

(38) Bouchelouche, K.; Capala, J.; Oehr, P. Positron emission tomography/computed tomography and radioimmunotherapy of prostate cancer. *Curr. Opin. Oncol.* **2009**, *21*, 469–474.

(39) Milowsky, M. I.; Nanus, D. M.; Kostakoglu, L. Vascular targeted therapy with anti-prostate-specific membrane antigen monoclonal antibody J591 in advanced solid tumors. *J. Clin. Oncol.* **2007**, *25*, 540–547.

(40) Byun, Y.; Mease, R. C.; Lupold, S. E.; Pomper, M. G. In *Drug Design of Zinc-Enzyme Inhibitors: Functional, Structural, and Disease Applications*; Supuran, C. T., Winum, J.-Y., Eds.; Binghe Wang Wiley Series in Drug Discovery and Development; John Wiley and Sons: Hoboken, NJ, 2009; pp 881−910.

(41) Zhou, J.; Neale, J. H.; Pomper, M. G.; Kozikowski, A. P. NAAG peptidase inhibitors and their potential for diagnosis and therapy. *Nat. Rev. Drug Discovery* **2005**, *4*, 1015–1026.

(42) Maresca, K. P.; Hillier, S. M.; Femia, F. J.; Keith, D.; Barone, C.; Joyal, J. L.; Zimmerman, C. N.; Kozikowski, A. P.; Barrett, J. A.; Eckelman, W. C.; et al. A series of halogenated heterodimeric inhibitors of prostate specific membrane antigen (PSMA) as radiolabeled probes for targeting prostate cancer. *J. Med. Chem.* **2009**, *52*, 347–357.

(43) Sanna, V.; Pintus, G.; Roggio, A. M.; Punzoni, S.; Posadino, A. M.; Arca, A.; Marceddu, S.; Bandiera, P.; Uzzau, S.; Sechi, M. Targeted Biocompatible Nanoparticles for the Delivery of (-)-Epigallocatechin 3-Gallate to Prostate Cancer Cells. *J. Med. Chem.* **2011**, *54*, 1321–1332.

(44) Yang, F.; Gu, A.; Chen, Z.; Gu, N.; Ji, M. Multiple emulsion microbubbles for ultrasound imaging. *Mater. Lett.* **2008**, *62*, 121–124.

(45) Yang, F.; Li, Y.; Chen, Z.; Zhang, Y.; Wu, J.; Gu, N. Superparamagnetic iron oxide nanoparticle-embedded encapsulated microbubbles as dual contrast agents of magnetic resonance and ultrasound imaging. *Biomaterials* **2009**, *30*, 3882–3890.

(46) Pasciu, V.; Posadino, A. M.; Cossu, A.; Sanna, B.; Tadolini, B.; Gaspa, L.; Marchisio, A.; Dessole, S.; Capobianco, G.; Pintus, G. Akt downregulation by flavin oxidase-induced ROS generation mediates dose-dependent endothelial cell damage elicited by natural antioxidants. *Toxicol. Sci.* **2010**, *114*, 101–112.

(47) Avgoustakis, K. Pegylated poly(lactide) and poly(lactide-co-glycolide) nanoparticles: preparation, properties and possible applications in drug delivery. *Curr. Drug Delivery* **2004**, *1*, 321–333.

(48) Gref, R.; Luck, M.; Quellec, P.; Marchand, M.; Dellacherie, E.; Harnisch, S.; Blunk, T.; Muller, R. H. Stealth" corona-core nanoparticles surface modified by polyethylene glycol (PEG): influences of the corona (PEG chain length and surface density) and of the core composition on phagocytic uptake and plasma protein adsorption. *Colloids Surf., B* **2000**, *18*, 301–313.

(49) Schülke, N.; Varlamova, O. A.; Donovan, G. P.; Ma, D.; Gardner, J. P.; Morrissey, D. M.; Arrigale, R. R.; Zhan, C.; Chodera, A. J.; Surowitz, K. G.; Maddon, P. J.; Heston, W. D.; Olson, W. C. The homodimer of prostate-specific membrane antigen is a functional target for cancer therapy. *Proc. Natl. Acad. Sci. U.S.A.* **2003**, *100*, 12590–12595.

(50) Mesters, J. R.; Barinka, C.; Li, W.; Tsukamoto, T.; Majer, P.; Slusher, B. S.; Konvalinka, J.; Hilgenfeld, R. Structure of glutamate carboxypeptidase II, a drug target in neuronal damage and prostate cancer. *EMBO J.* **2006**, *25*, 1375–1384.

(51) Gu, F.; Zhang, L.; Teply, B. A.; Mann, N.; Wang, A.; Radovic-Moreno, A. F.; Langer, R.; Farokhzad, O. C. Precise engineering of targeted nanoparticles by using self-assembled biointegrated block copolymers. *Proc. Natl. Acad. Sci. U.S.A.* **2008**, *105*, 2586–2591.

(52) Betancourt, T.; Byrne, J. D.; Sunaryo, N.; Crowder, S. W.; Kadapakkam, M.; Patel, S.; Casciato, S.; Brannon-Peppas, L. PEGylation strategies for active targeting of PLA/PLGA nanoparticles. *J. Biomed. Mater. Res. A.* **2009**, *91*, 263–276.

(53) El-Sherif, D. M.; Lathia, J. D.; Le, N. T.; Wheatley, M. A. Ultrasound degradation of novel polymer contrast agents. *J. Biomed. Mater. Res. A.* **2004**, *68*, 71–78.

(54) Rosca, I. D.; Watari, F.; Uo, M. Microparticle formation and its mechanism in single and double emulsion solvent evaporation. *J. Controlled Release* **2004**, *99*, 271–280.

(55) Morgan, K. E.; Allen, J. S.; Dayton, P. A.; Chomas, J. E.; Klibanov, A. L.; Ferrara, K. W. Experimental and theoretical evaluation of microbubble behavior: Effect of transmitted phase and bubble size. *IEEE Trans. Ultrason., Ferroelectr. Freq. Control* **2000**, *47*, 1494–1509.

(56) Banerjee, S. R.; Foss, A. C.; Castanares, M.; Mease, R. C.; Byun, Y.; Fox, J. J.; Hilton, J.; Lupold, S. E.; Kozikowski, A. P.; Pomper, M. G. Synthesis and evaluation of technetium-99m- and rhenium-labeled inhibitors of the prostate-specific membrane antigen (PSMA). *J. Med. Chem.* **2008**, *51*, 4504–4517.

(57) Maclaren, J. A. Some amino acid esters-an improved preparative method. *Aust. J. Chem.* **1978**, *31*, 1865–1868.

(58) Cheng, J.; Teply, B. A.; Sherifi, I.; Sung, J.; Luther, G.; Gu, F. X.; Levy-Nissenbaum, E.; Radovic-Moreno, A. F.; Langer, R.; Farokhzad, O. C. Formulation of functionalized PLGA-PEG nanoparticles for in vivo targeted drug delivery. *Biomaterials* **2007**, *28*, 869–876.

(59) Dhar, S.; Gu, F. X.; Langer, R.; Farokhzad, O. C.; Lippard, S. J. Targeted delivery of cisplatin to prostate cancer cells by aptamer functionalized Pt(IV) prodrug-PLGA-PEG nanoparticles. *Proc. Natl. Acad. Sci. U.S.A.* **2008**, *105*, 17356–17361.